Deep Space Telecommunications and the Solar Cycle: A Reappraisal

A. L. Berman
TDA Engineering Office

Observations of density enhancement in the near corona ($r \leqslant 5r_\odot$) at solar cycle (sunspot) maximum have rather uncritically been interpreted to apply equally well to the extended corona ($r \geqslant 5r_\odot$), thus generating concern about the quality of outer planet navigational data at solar cycle maximum. Spacecraft have been deployed almost continuously during the recently completed solar cycle 20, providing two powerful new coronal investigatory data sources: (1) in-situ spacecraft plasma measurements at approximately 1 AU, and (2) plasma effects on monochromatic spacecraft signals at all signal closest approach points.

A comprehensive review of these (solar cycle 20) data leads to the somewhat surprising conclusion that for the region of interest of navigational data ($r \geqslant 30r_\odot$), the highest levels of charged-particle corruption of navigational data can be expected to occur at solar cycle minimum, rather than solar cycle maximum, as previously believed.

I. Introduction

A modern view of electron density in the near corona (here to be defined as $r \leqslant 5r_\odot$, where r is the solar radial distance and $r_\odot$ is the solar radius) begins with the careful eclipse white light photometry analysis of van de Hulst in the late 1940s (Refs. 1 and 2). The white light corona is composed of two primary components, the K corona, resulting from Thompson scattering by free electrons, and the F corona (zodiacal light), resulting from scattering by interplanetary dust. Van de Hulst made various assumptions which allowed him to separate out the F corona, and hence obtain the K corona, or the desired near corona electron density. As part of this exercise, van de Hulst adopted a value of 1.8 for the ratio of solar (sunspot) cycle maximum equatorial electron density to solar (sunspot) cycle minimum equatorial electron density, based on coronal brightness comparisons (eclipse photometry) between solar cycle maximum and minimum. At about the same time, Saito (see Billings, Ref. 3), also working to obtain coronal electron density, deduced a similar value of approximately 2.0 for the solar cycle ratio (subsequently in this report, the term "solar cycle ratio" will be defined for a given parameter as the parameter (average) value at solar cycle maximum divided by the parameter (average) value at solar cycle minimum).

Since that time, a number of coronal investigators, performing eclipse photometry analysis, have obtained similar near corona equatorial electron density solar cycle ratios. For instance, the composite eclipse photometry analysis by Blackwell, et al. (Ref. 4) produced a solar cycle ratio of 1.9 ($2_\odot$). A consensus of eclipse photometry, radio interferometry, and radio scattering experiments into the mid-1960s (Newkirk,

Ref. 5) produced a solar cycle ratio for near corona electron density of approximately 2.0. More recently, Hansen et al. (Ref. 6), using a K coronameter to investigate the near corona region under $2r_\odot$ on a daily basis during the ascendant portion of solar cycle 20 (1964 to 1967), convincingly confirmed the near corona solar cycle ratio of approximately 2.0.

The observed density enhancement of the near corona at solar cycle maximum has (not surprisingly!) come to be applied to the extended corona (here defined as $r \gtrsim 5r_\odot$) as well, to the point where it is now considered axiomatic that the highest electron densities (and density fluctuations) in the extended corona occur at solar cycle maximum. This assumption has resulted in an elevated level of anxiety about navigational data (doppler and range) quality[1] during the upcoming (1979-1981) solar cycle 21 maximum. There exists particular concern about radiometric data quality during the pre-Saturn encounter periods for both Pioneer 11 and Voyager.

Prior to the start of solar cycle 20 (1964), the main tools available for coronal electron density investigation were white light eclipse photometry, K coronameter, and natural radio source scattering (principally of the Crab Nebula). However, the advent of solar cycle 20 marked the near continuous deployment of deep space probes (both Earth orbiters beyond the magnetosphere and planetary probes), offering two new incredibly powerful coronal investigatory tools:

(1) In-situ plasma measurements at approximately 1 AU

(2) Columnar measurements over all signal closest approach points of the plasma effects on a monochromatic spacecraft signal

A comprehensive review of both types of spacecraft measurements made during the full extent of solar cycle 20 reveals startling results which strongly contradict the "conventional wisdom" concerning enhanced density in the extended corona during solar cycle maximum, these results being:[2]

Density region (equatorial)	Solar cycle ratio
Near corona ($r \lesssim 5r_\odot$)	~2.0
Extended corona ($r \gtrsim 5r_\odot$)	
$r = 10r_\odot$	~1.0
$r = 1$ AU	~0.65

[1] A detailed derivation and description of the effect of free electrons on doppler and range can be found in MacDoran, Ref. 7.

[2] Note that these results are in no way contradictory. For instance, if the particle flux were assumed constant with solar cycle, all that is required is a change in the radial solar wind velocity signature with solar cycle, as is sketched in Fig. 1.

For radio metric (navigational) data quality, the $10r_\odot$ to 1 AU results are the most important, and indicate (if solar cycle 21 proves similar to solar cycle 20):

(1) Electron density (and density fluctuations) between $10r_\odot$ and 1 AU can be expected to stay roughly the same ($10r_\odot$) or decrease (1 AU) between now and approximately 1981.

(2) The extensive doppler phase fluctuation work done during the 1975 to 1976 solar cycle 20 minimum (Refs. 8–18), should provide an *upper bound* for the expected radio metric data plasma corruption over the next solar cycle.

The following sections will describe the solar cycle variations (in both mean value and fluctuation) of electron density (at $10r_\odot$ and 1 AU), solar wind velocity at 1 AU, particle flux at 1 AU, and the columnar density fluctuation spectral index.

II. Solar Wind Variations With Solar Cycle at 1 AU

As mentioned in Section I, many deep space probes have been deployed since the beginning of solar cycle 20 (1964), particularly Earth orbiters (beyond the magnetosphere) at approximately 1 AU. The major obstacle in utilizing the resultant in-situ plasma measurements is that each spacecraft has separate systematic errors (bias and linear) in each of the parameters measured (density, wind velocity, etc.), hence it would be of dubious value to compare the "unnormalized" plasma measurements from the 10 plus spacecraft needed to span the solar cycle 20 time frame. Fortunately, the problem of spacecraft intercalibration has been addressed by Diodato, et al. (ref. 19) who have intercalibrated in-situ plasma measurements for a number of Earth orbiters during the period 1965 to 1971. The process of intercalibrating spacecraft is in itself subject to error, as is discussed by M. Neugebauer (Ref. 20); however, the Diodato data are the best available and are expected to provide a reasonably valid picture. The Diodato data will be utilized to examine the variation of density and particle flux with the solar cycle. For solar wind velocity variations with solar cycle, the recent and significantly more encompassing work of Gosling, et al. (Ref. 21), will be utilized.[3]

The basic format of the data will be presentations in bar graph form of various parameter yearly averages, as compared to the observed sunspot number during the same time frame.

[3] Intercalibration of spacecraft solar wind velocity measurements is a considerably less severe problem than for density measurements (on a percentage basis).

A. Proton Density

Although electron density is the parameter of interest in regard to navigational data quality, the approximate equality between solar wind electrons and protons allows the usage of proton density for the same purpose. The slight difference between the two occurs because of the presence of a small amount of helium in the solar wind; Ogilvie, et al. (Ref. 22) shows the helium presence, although correlated with solar cycle, to be only about 4% ± 0.5% (of hydrogen) over the solar cycle, and hence not particularly significant to the overall density picture. The density parameters from Diodato, with the exception of Fig. 5 which is from M. Neugebauer (Ref. 23), are:

Figure 2. Proton density yearly average at 1 AU, 1965–1971

Figure 3. Proton fluctuation density yearly average at 1 AU, 1965–1971

Figure 4. Proton fluctuation to density ratio, yearly average from 1965–1971, at 1 AU

Figure 5. Long-term averages of fractional time density > 10 cm^{-3} at 1 AU, from 1962–1972

Examination of Fig. 2 clearly indicates a pronounced (anti) correlation of density with solar cycle. The data in Fig. 2 indicate a solar cycle ratio of approximately 0.65. Feldman, et al. (Ref. 24) give more recent density information from the Imp spacecraft as follows:

1972/1973 average (Imp 7): $N_p = 9.0$ cm^{-3}

1973/1974 average (Imp 8): $N_p = 11.3$ cm^{-3}

Even allowing for a possible 10 to 20% calibration difference, these numbers clearly continue the strong trend of Fig. 2.

Figure 3 shows the same solar cycle anticorrelation for the average yearly density fluctuation (standard deviation); the solar cycle ratio is again approximately 0.65. The Feldman, et al. Imp 7 and 8 density fluctuation numbers are:

1972/1973 average: $\sigma(N_p) = 4.3$ cm^{-3}

1973/1974 average: $\sigma(N_p) = 5.4$ cm^{-3}

continuing the same pronounced trend in the density fluctuation as in the (mean) density itself.

The ratio of density fluctuation to (mean) density as seen in Fig. 4 does not show a clear trend with solar cycle; the average value for this parameter over the seven year period 0.56. The corresponding Feldman et al. numbers are:

1972/1973 average: $\epsilon = 0.48$

1973/1974 average: $\epsilon = 0.48$

Finally, Fig. 5 (from Neugebauer, Ref. 23), which presents long-term averages of fractional time density > 10 cm^{-3}, and encompasses a greater number of spacecraft and a longer time frame (than the Diodato data), corroborates and strengthens the density fluctuation data presented in Fig. 3. Figure 5 is a most dramatic view of the pronounced anticorrelation of density and density fluctuation with solar cycle at 1 AU, and indicates that the corruption of navigational data (at least in the general vicinity of 1 AU) will be highest at solar cycle minimum, and lowest at solar cycle maximum, both in regard to range errors (density) and doppler errors (density fluctuation).

B. Proton Flux

The proton (particle) flux data from Diodato is presented as follows:

Figure 6. Proton flux yearly average at 1 AU, 1965 to 1971

Figure 7. Proton fluctuation flux yearly average at 1 AU, 1965 to 1971

Figure 8. Proton flux fluctuation to flux ratio, yearly average from 1965 to 1971, at 1 AU

These proton flux data very much pattern the behavior of the equivalent proton density parameters, which is mostly a reflection that the solar wind velocity is far more stable (percentage wise) with the solar cycle than is density. The solar cycle ratio of proton flux is 0.7, while for flux fluctuation it is 0.65. The average ratio of flux fluctuation to flux is approximately 0.52, or slightly lower than the equivalent density ratio.

C. Solar Wind Radial Velocity

Solar wind radial velocity from Gosling, et al. is presented as follows:

Figure 9. Solar wind radial velocity yearly average at 1 AU, 1964 to 1974

Figure 10. Solar wind fluctuation radial velocity yearly average at 1 AU, 1964 to 1974

Figure 11. Solar wind velocity fluctuation to velocity ratio, yearly average from 1964 to 1974, at 1 AU

In sharp contrast to the density and flux at 1 AU, it is difficult to discern a clear variation of solar wind velocity with solar cycle; of the three years of significantly enhanced velocity (1968, 1973, 1974), one occurs at solar cycle maximum and

two occur during the declining portion of the cycle, near to solar cycle minimum. If one is forced to make a decision, one would have to decide in favor of anticorrelation with the solar cycle, albeit much less pronounced than that displayed by density and flux. Gosling et al. were much more firm in this conviction (i.e., of definite anticorrelation) based on their data.[4] At any rate, the solar cycle ratio for the radial velocity would seem to be at least 0.8. Somewhat strangely, the radial velocity fluctuation data seen in Fig. 10 demonstrate a much more pronounced anticorrelation with solar cycle; the solar cycle ratio for radial velocity fluctuation is 0.7. Finally, the ratio of velocity fluctuation to (mean) velocity averages about 0.17, or only about 30% of the equivalent density parameter.

III. Electron Density Variation With Solar Cycle at $r = 10r_\odot$

Even as solar cycle 20 was beginning in the mid-1960s, there was information available which suggested that the near corona density enhancement observed at solar cycle maximum did not necessarily apply to the extended corona. The eclipse photometry of Blackwell is summarized by Anderson (Ref. 29) as follows:

Solar cycle maximum:

$$N_e(r) = \frac{2.62 \times 10^8}{r^6} + \frac{2.07 \times 10^6}{r^{2.33}}, \text{cm}^{-3}$$

Solar cycle minimum:

$$N_e(r) = \frac{1.01 \times 10^8}{r^6} + \frac{2.01 \times 10^6}{r^{2.33}}, \text{cm}^{-3}$$

Although the near corona solar cycle ratio is approximately 2.6, the values of the Blackwell models at $r = 10r_\odot$ are:

Solar cycle maximum: $N_e(10r_\odot) = 9940\ \text{cm}^{-3}$

Solar cycle minimum: $N_e(10r_\odot) = 9500\ \text{cm}^{-3}$

or virtually no variation with solar cycle at $r = 10r_\odot$. Since the mid-1960s, a number of experiments have been conducted to (indirectly) measure and subsequently model electron density in the extended corona. These experiments have utilized either spacecraft signals or natural sources (primarily pulsars) as these signals passed through a wide variation of signal closest approach points. The measurements yield total columnar density, which is then mapped back to a radially dependent density model after making suitable assumptions. Table 1 presents these models as evaluated at $r = 10r_\odot$; the same data appear in Fig. 12. Examination of Fig. 12 indicates no significant correlation with solar cycle. Although the data appear sparse at first glance, it is important to bear in mind that in most cases each point represents the distillation of copious amounts of data taken over weeks or months; still, a better determination of the solar cycle variation of density at $r = 10r_\odot$ will have to await the expected high quality dual frequency range results of the Viking and Voyager spacecraft.

IV. Variation of the Columnar Fluctuation Spectral Index With the Solar Cycle

The columnar fluctuation spectral index is based on the commonly accepted assumption for a power law form of the columnar (two-dimensional) fluctuation spectrum:

$$P(\nu) = K_1 \nu^{-K_0}$$

where

P = columnar fluctuation spectrum

ν = fluctuation frequency

K_0 = spectral index

The significance of the spectral index is that, given the same level of low frequency (long time scale) fluctuation, a larger spectral index yields a smaller amount of high frequency (short time scale) fluctuation (i.e., the fluctuations "fall off" more rapidly with increasing frequency). Experiments have been performed to measure the in situ (one dimensional) density fluctuation spectrum as well as the columnar fluctuation spectrum; the two spectral indices are related (Cronyn, Ref. 34) via the relationship:

$$(K_0)_{\text{columnar}} = (K_0)_{\text{in situ}} + 1$$

Table 2 and Fig. 13 present the columnar fluctuation spectral indices as well as in situ "equivalents"; examination of Fig. 13 reveals no clear or significant variation with solar cycle. The data (points) are quite sparse, but again, each point represents a large amount of processed data, spanning time periods of several days to several months. If pressed, one would have to say that the spectral index looks to be slightly larger (steeper) at solar cycle maximum, indicating a more rapid falloff of

[4] An additional piece of data not shown in Fig. 9 is a (high) yearly average radial velocity of 489 km/s for 1962, which is a near solar cycle minimum year. With this additional data, the case for significant anticorrelation is strengthened.

high frequency fluctuations during cycle maximum, and thus in consonance with the low frequency fluctuation data of Figs. 3 and 5.

Berman has reported (Ref. 15) a new technique and DSN capability which allows spectral index information to be easily extracted from routine doppler noise. If proven out, this new technique should allow voluminous amounts of spectral index data to be acquired during solar cycle 21, and analyzed for solar cycle variation.

V. Summary and Conclusions

Table 3 summarizes the relationship to solar cycle of the various parameters described in this report. For navigational usage of radiometric data, the most important region is $r \gtrsim 30 r_{\odot}$, or a Sun-Earth-probe angle $\gtrsim 8$ degrees. For this region, the experience at $r = 1$ AU ($215 r_{\odot}$) should be the most applicable. The 1 AU experience during solar cycle *maximum* which is most important to navigational data is:

Density	Strong minimum
Density fluctuation	Strong minimum
Fractional time	
Density $> 10\ \mathrm{cm}^{-3}$	Strong minimum
Velocity fluctuation	Moderate minimum
Spectral index	No change or weak maximum

Based on the above, solar cycle *maximum* would appear to yield the lowest level of charged-particle corruption of navigational data, and hence the placement of the Pioneer 11 and Voyager Saturn encounters (near solar cycle 21 maximum) may in fact prove close to optimum, rather than decidedly inopportune, as is currently considered.

References

1. van de Hulst, H. C., "The Electron Density of the Solar Corona," *Bulletin of the Astronomical Institutes of the Netherlands,* Volume XI, Number 410, February 2, 1950.
2. van de Hulst, H. C., "The Chromosphere and the Corona," in *The Sun*, edited by G. P. Kuiper, The University of Chicago Press, Chicago, Illinois, 1953.
3. Billings, D. E., *A Guide to the Solar Corona*, Academic Press, New York, London, 1966.
4. Blackwell, D. E., Dewhirst, D. W., and Ingham, M. F., *Advances in Astronomy and Astrophysics* 5, Academic Press, New York, 1967.
5. Newkirk, G., "Structure of the Solar Corona," in *The Annual Review of Astronomy and Astrophysics*, Vol. 5, 1967.
6. Hansen, R. T., Garcia, C. J., Hansen, S. F., and Loomis, H. G., "Brightness Variations of the White Light Corona During the Years 1964-1967," in *Solar Physics* 7, 1969.
7. MacDoran, P. F., "A First Principles Derivation of the Differenced Range versus Integrated Doppler (DRVID) Charged Particle Calibration Method," in *The Deep Space Network, Space Programs Summary 37-62,* Volume II, Jet Propulsion Laboratory, Pasadena, California, March 31, 1970.
8. Berman, A. L., and Wackley, J. A., "Doppler Noise Considered as a Function of the Signal Path Integration of Electron Density," in *The Deep Space Network Progress Report 42-33*, Jet Propulsion Laboratory, Pasadena, California, 15 June 1976.
9. Berman, A. L., Wackley, J. A., Rockwell, S. T., and Yee, J. G., "The Pioneer 11 1976 Solar Conjunction: A Unique Opportunity to Explore the Heliographic Latitudinal Variations of the Solar Corona," in *The Deep Space Network Progress Report 42-35*, Jet Propulsion Laboratory, Pasadena, California, 15 October 1976.

10. Berman, A. L., Wackley, J. A., and Rockwell, S. T., "The 1976 Helios and Pioneer Solar Conjunctions – Continuing Corroboration of the Link Between Doppler Noise and Integrated Signal Path Electron Density," in *The Deep Space Network Progress Report 42-36,* Jet Propulsion Laboratory, Pasadena, California, 15 December 1976.

11. Berman, A. L., "A Comprehensive Two-Way Doppler Noise Model for Near-Real-Time Validation of Doppler Data," in *The Deep Space Network Progress Report 42-37,* Jet Propulsion Laboratory, Pasadena, California, February 15, 1977.

12. Berman, A. L., and Wackley, J. A., "Viking S-Band Doppler RMS Phase Fluctuations Used to Calibrate the Mean 1976 Equatorial Corona," in *The Deep Space Network Progress Report 42-38,* Jet Propulsion Laboratory, Pasadena, California, 15 April 1977.

13. Berman, A. L., Wackley, J. A., Rockwell, S. T., and Kwan, M., "Viking Doppler Noise used to Determine the Radial Dependence of Electron Density in the Extended Corona," in *The Deep Space Network Progress Report 42-38,* Jet Propulsion Laboratory, Pasadena, California, April 15, 1977.

14. Berman, A. L., "Proportionality Between Doppler Noise and Integrated Signal Path Electron Density Validated by Differenced S-X Range," in *The Deep Space Network Progress Report 42-38,* Jet Propulsion Laboratory, Pasadena, California, April 15, 1977.

15. Berman, A. L., "Phase Fluctuation Spectra: New Radio Science Information to Become Available in the DSN Tracking System Mark III-77," in *The Deep Space Network Progress Report 42-40,* Jet Propulsion Laboratory, Pasadena, California, August 15, 1977.

16. Berman, A. L., "Electron Density in the Extended Corona: Two Views," in *The Deep Space Network Progress Report 42-41,* Jet Propulsion Laboratory, Pasadena, California, October 15, 1977.

17. Berman, A. L., "An Empirical Model for the Solar Wind Velocity," in *The Deep Space Network Progress Report 42-42,* Jet Propulsion Laboratory, Pasadena, California, December 15, 1977.

18. Berman, A. L., "RMS Electron Density Fluctuation at 1 AU," in *The Deep Space Network Progress Report 42-42,* Jet Propulsion Laboratory, Pasadena, California, December 15, 1977.

19. Diodato, L., Moreno, G., Signorini, C., and Ogilvie, K. W., "Long Term Variations of the Solar Wind Proton Parameters," in *The Journal of Geophysical Research,* Volume 79, Number 34, Dec. 1, 1974.

20. Neugebauer, M., "The Quiet Solar Wind," in *The Journal of Geophysical Research,* Volume 81, Number 25, September 1, 1976.

21. Gosling, J. T., Asbridge, J. R., Bame, S. J., and Feldman, W. C., "Solar Wind Speed Variations: 1962–1974," *Journal of Geophysical Research,* Volume 81, Number 28, October 1, 1976.

22. Ogilvie, K. W., and Hirshberg, J., "The Solar Cycle Variation of the Solar Wind Helium Abundance," in *The Journal of Geophysical Research,* Volume 79, Number 31, November 1, 1974.

23. Neugebauer, M., "Large-Scale and Solar-Cycle Variations of the Solar Wind," in *Space Science Reviews* 17, 1975.

24. Feldman, W. C., Asbridge, J. R., Bame, S. J., Montgomery, M. D., and Gary, S. P., "Solar Wind Electrons," in *The Journal of Geophysical Research*, Volume 80, Number 31, November 1, 1975.

25. Edenhofer, P., Esposito, P. B., Hansen, R. T., Hansen, S. F., Lüneburg, E., Martin, W. L., and Zygielbaum, A. I., "Time Delay Occultation Data of the Helios Spacecrafts and Preliminary Analysis for Probing the Solar Corona," in the *Journal of Geophysics* 42, 1977.

26. Weisberg, J. M., Rankin, J. M., Payne, R. R., and Counselman III, C. C., "Further Changes in the Distribution of Density and Radio Scattering in the Solar Corona," *The Astrophysical Journal*, Volume 209, October 1, 1976.

27. Anderson, J. D., Keesey, M. S. W., Lau, E. L., Standish, E. M., Jr., and Newhall, X. X., "Tests of General Relativity using Astrometric and Radiometric Observations of the Planets," Third International Space Relativity Symposium, International Astronautical Federation, XXVII Congress, Anaheim, October, 1976.

28. Counselman III, C. C., and Rankin, J. M., "Density of the Solar Corona from Occultations of NP0532," *The Astrophysical Journal*, Volume 175, August 1, 1972.

29. Anderson, J. D., Esposito, P. B., Martin, W. L., Thornton, C. L., and Muhleman, D. O., "Experimental Test of General Relativity Using Time Delay Data from Mariner 6 and Mariner 7," in *The Astrophysical Journal*, Volume 200, August 15, 1975.

30. Woo, R., Yang, F., Yip, W. K., and Kendall, W. B., "Measurements of Large Scale Density Fluctuations in the Solar Wind Using Dual Frequency Phase Scintillations," in *The Astrophysical Journal*, Volume 210, Number 2, Part 1, December 1, 1976.

31. Unti, T. W. J., Neugebauer, M., and Goldstein, B. E., "Direct Measurement of Solar Wind Fluctuations Between 0.0048 and 13.3 Hz," in *The Astrophysical Journal*, 180, March 1, 1973.

32. Goldstein, B., and Sisco, G. L., "Spectra and Cross Spectra of Solar Wind Parameters From Mariner 5," in *Solar Wind*, edited by Sonett, C. P., Coleman, P. J., Jr., and Wilcox, J. M., National Aeronautics and Space Administration, Washington, D.C., 1972.

33. Intriligator, D. S., and Wolfe, J. H., "Preliminary Power Spectra of the Interplanetary Plasma," in *The Astrophysical Journal, Letters*, 162, December 1970.

34. Cronyn, W. M., "Density Fluctuations in the Interplanetary Plasma: Agreement Between Space Probe and Radio Scattering Observations," *Astrophysical Journal*, Volume 171, February 1,1972.

Table 1. Electron Density Model Evaluations at $r = 10r_{\odot}$

Source	Reference	Time (center) of observations	Equatorial density, cm^{-3}	Type of experiment
Berman et al.	12	9–76	8610	VK doppler noise
Berman et al.	12	6–76	8190	PN, HE doppler noise
Edenhofer et al.	25	4–76	6340	HE, S-band range
Berman et al.	8,14	6–75	7080	PN, HE doppler noise
Weisberg et al.	26	6–73	8000[a]	Pulsar time delay
Anderson et al.	27	9–72	7500	MA9 S-band range
Counselman et al.	28	6–71	8400[b]	Pulsar time delay
Blackwell et al.	29	7–63	7440	Eclipse photometry

[a]One of several solutions. This solution in best agreement with average in situ density values at 1 AU.

[b]One of several solutions. This solution included heliographic latitude.

Table 2. Columnar (two-dimensional) fluctuation spectral index

Source	Reference	Time (center) of observations	Index	Type of experiment
Berman	11,15	10–76	2.41	VK doppler noise
Berman	11,15	5–76	2.43	HE doppler noise
Woo et al.	30	5–74	2.55	MVM S–X doppler
Unti et al.	31	3–68	2.55[a]	OGO 5 in situ density
Goldstein et al.	32	9–67	2.3[a]	MA 5 in situ density
Intriligator et al.	33	1–66	2.3[a]	PN 6 in situ density

[a]In situ "equivalent"; converted via the relationship columnar index ≡ in situ index + 1.

Table 3. Summary of parameter correlation with solar cycle

Parameter	Correlation appearance	Solar cycle ratio	Solar cycle phase
Density			
Near corona ($r \leqslant 5r_{\odot}$)	Strong	~2.0	Positive
$r = 10r_{\odot}$	None	–	–
$r = 1$ AU	Strong	~0.65	Negative
Density fluctuation 1 AU	Strong	~0.65	Negative
Fluctuation/density ratio 1 AU	Weak	–	–
Flux 1 AU	Strong	~0.70	Negative
Flux fluctuation 1 AU	Strong	~0.65	Negative
Fluctuation/flux ratio 1 AU	Moderate	~0.75	Negative
Radial velocity 1 AU	Weak	>0.8	Negative
Velocity fluctuation 1 AU	Moderate	~0.70	Negative
Fluctuation/velocity ratio 1 AU	Moderate	~0.75	Negative
Fluctuation spectral index	Weak/none	–	–

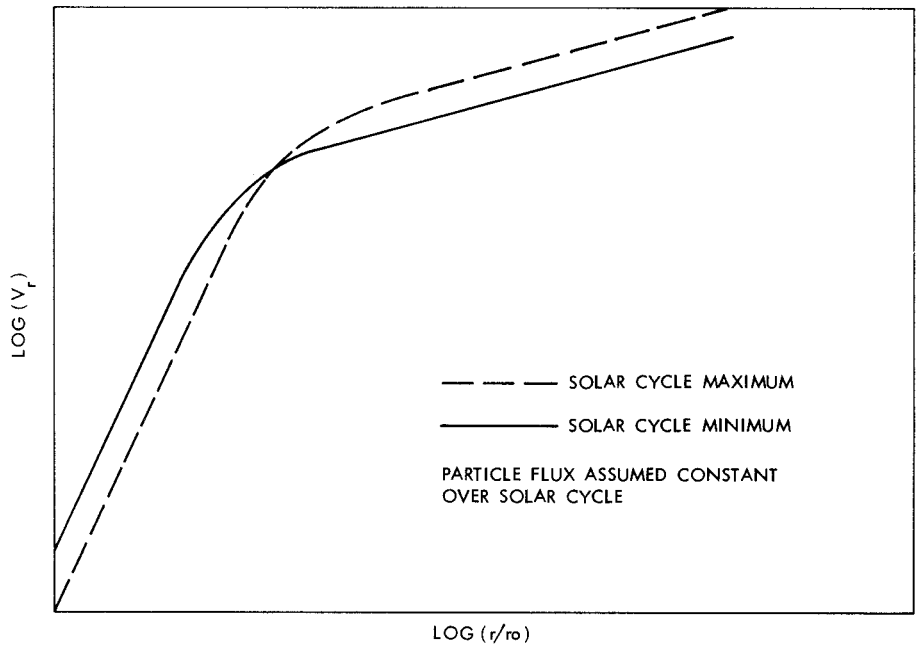

Fig. 1. Possible solar wind velocity signature with solar cycle

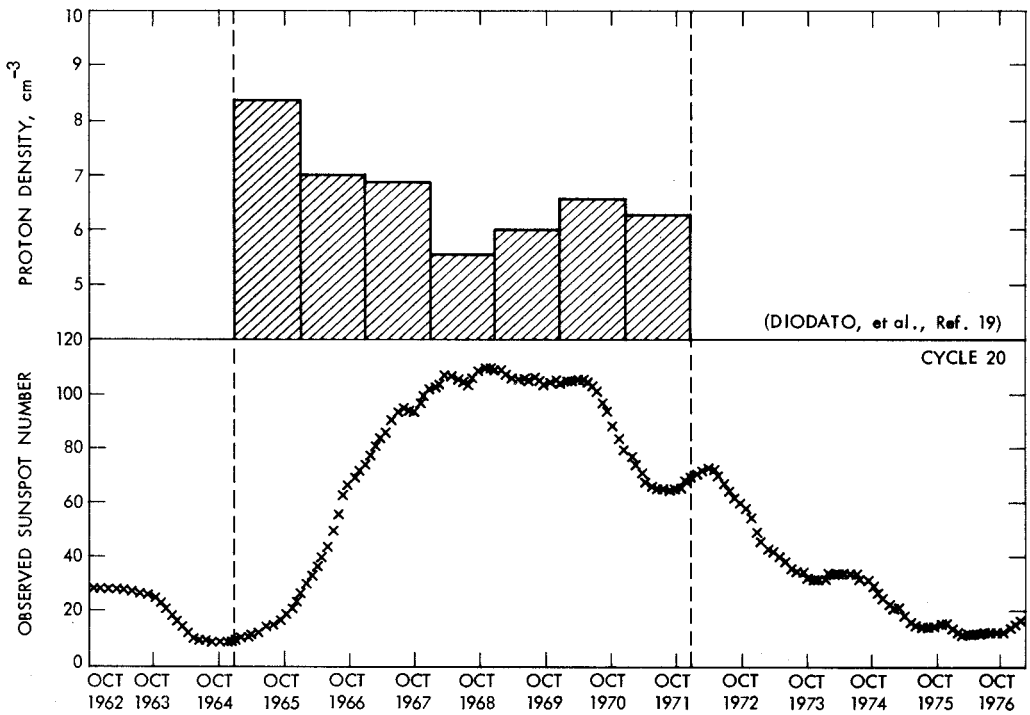

Fig. 2. Proton density yearly average at 1 AU, 1965 to 1971

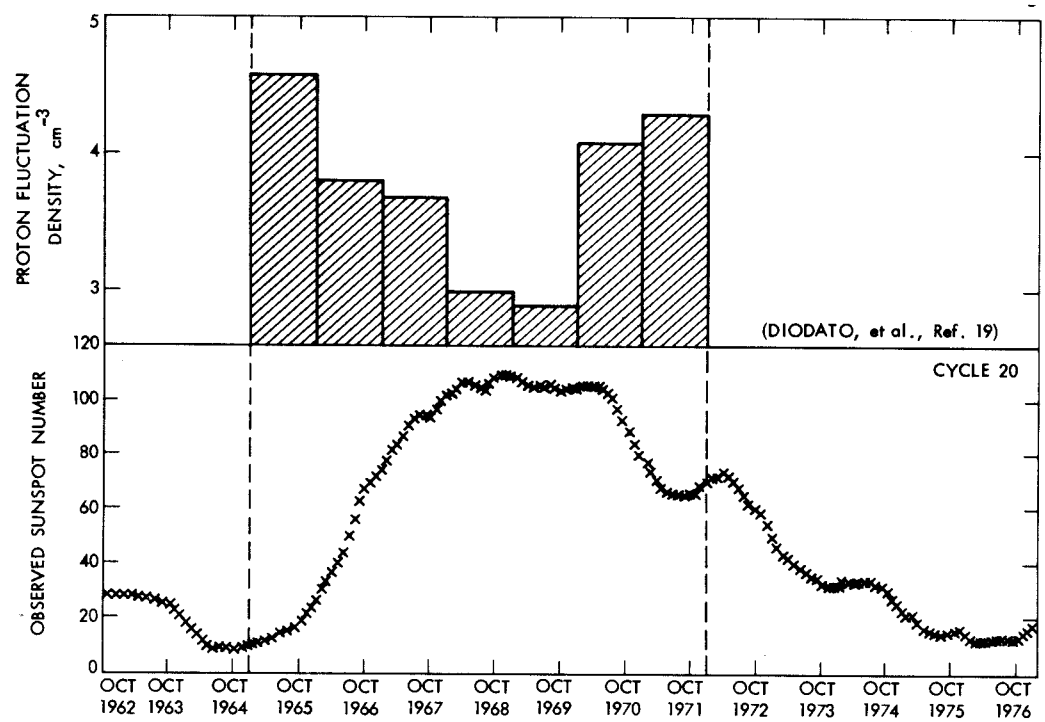

Fig. 3. Proton fluctuation density yearly average at 1 AU, 1965 to 1971

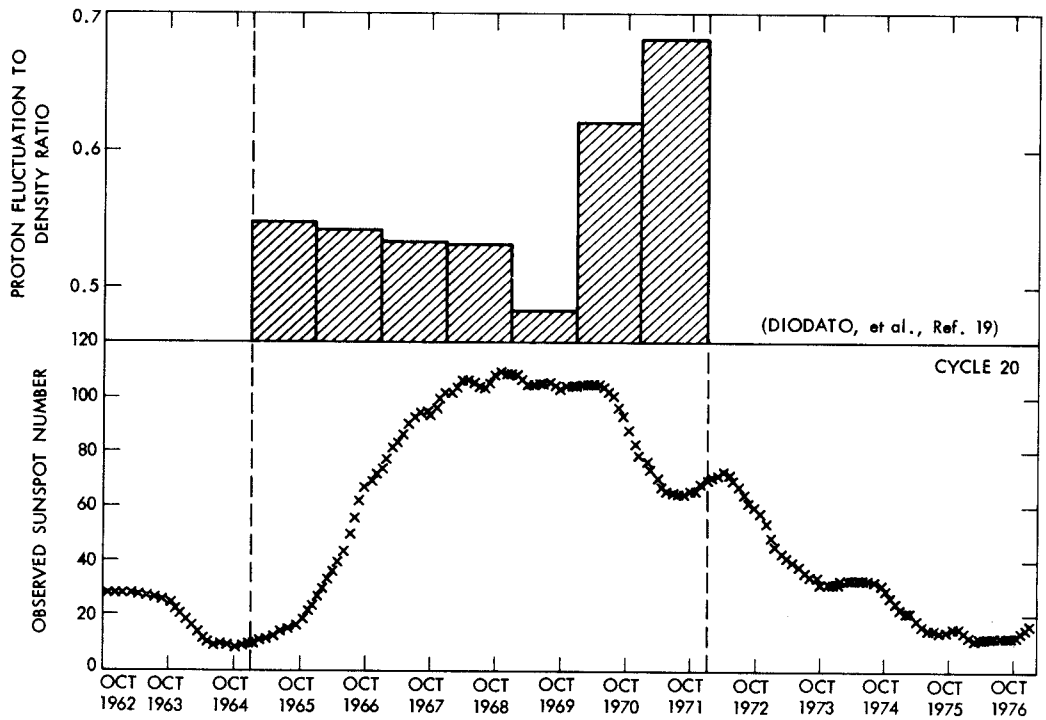

Fig. 4. Proton fluctuation to density ratio, yearly average from 1965 to 1971, at 1 AU

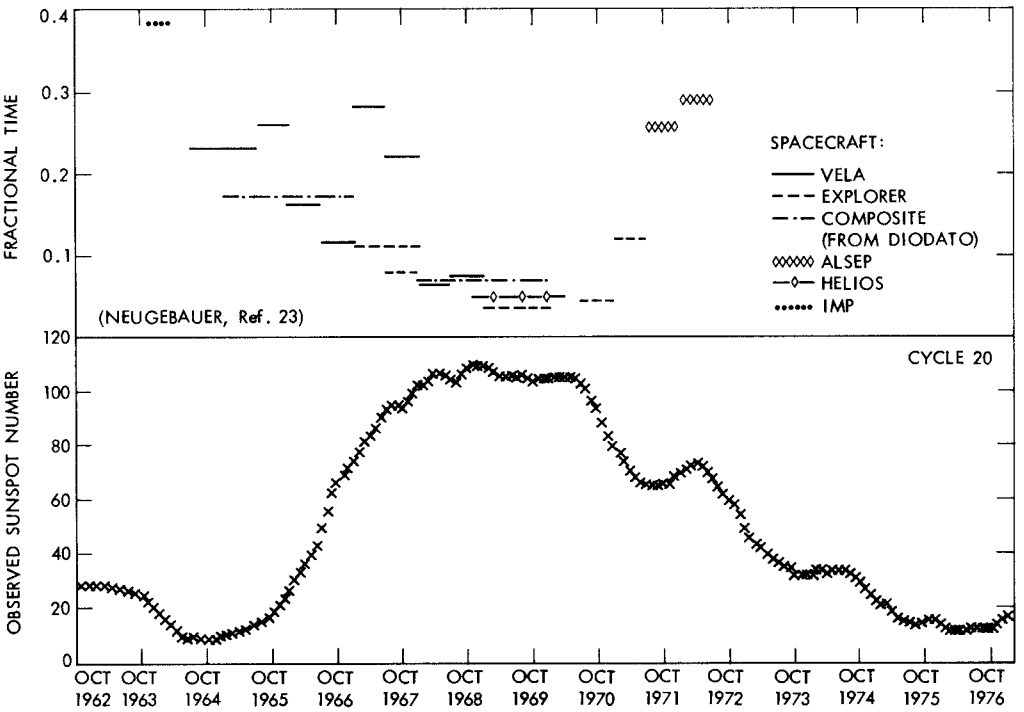

Fig. 5. Fractional time proton density observed greater than 10 cm^{-3}, at 1 AU

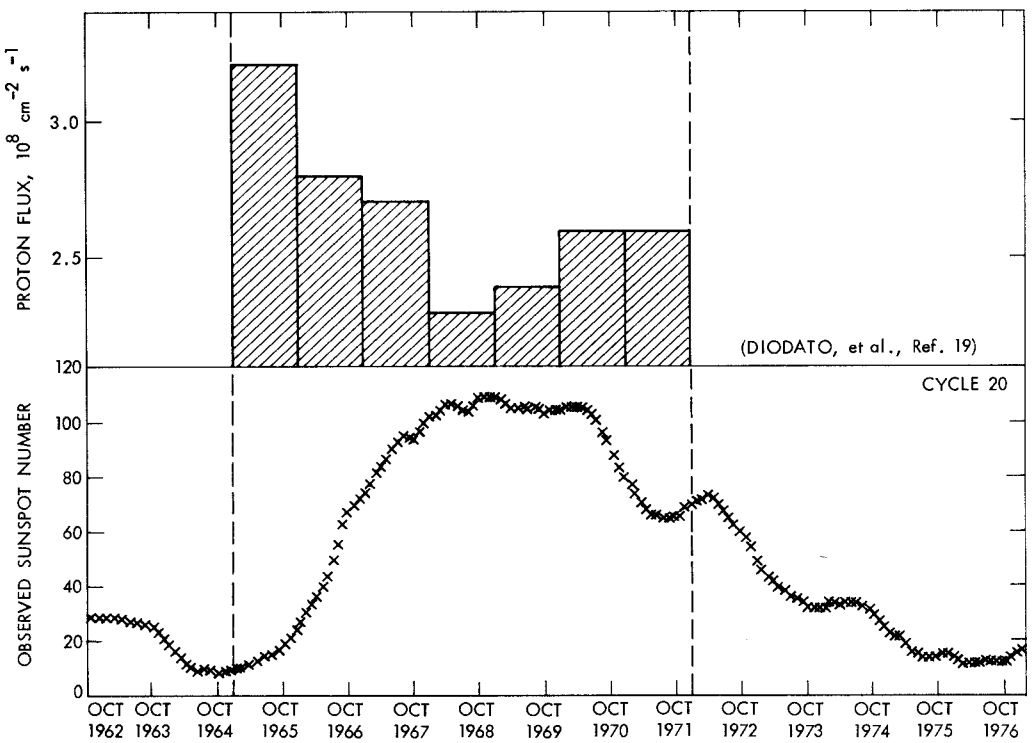

Fig. 6. Proton flux yearly average at 1 AU, 1965 to 1971

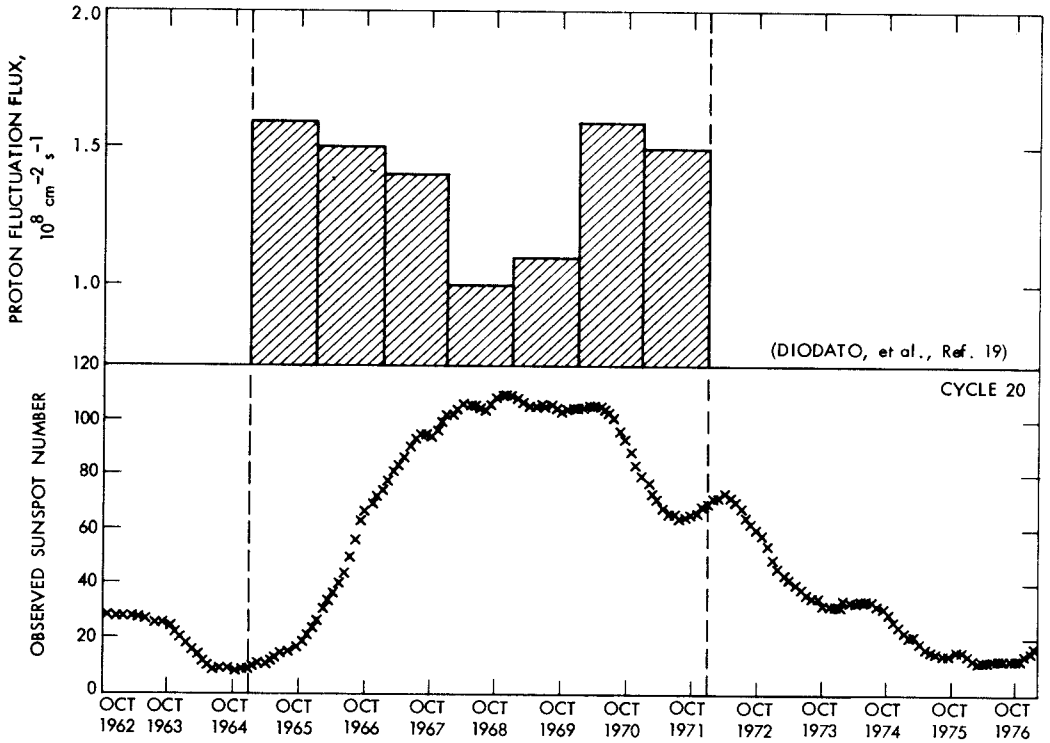

Fig. 7. Proton fluctuation flux yearly average at 1 AU, 1965 to 1971

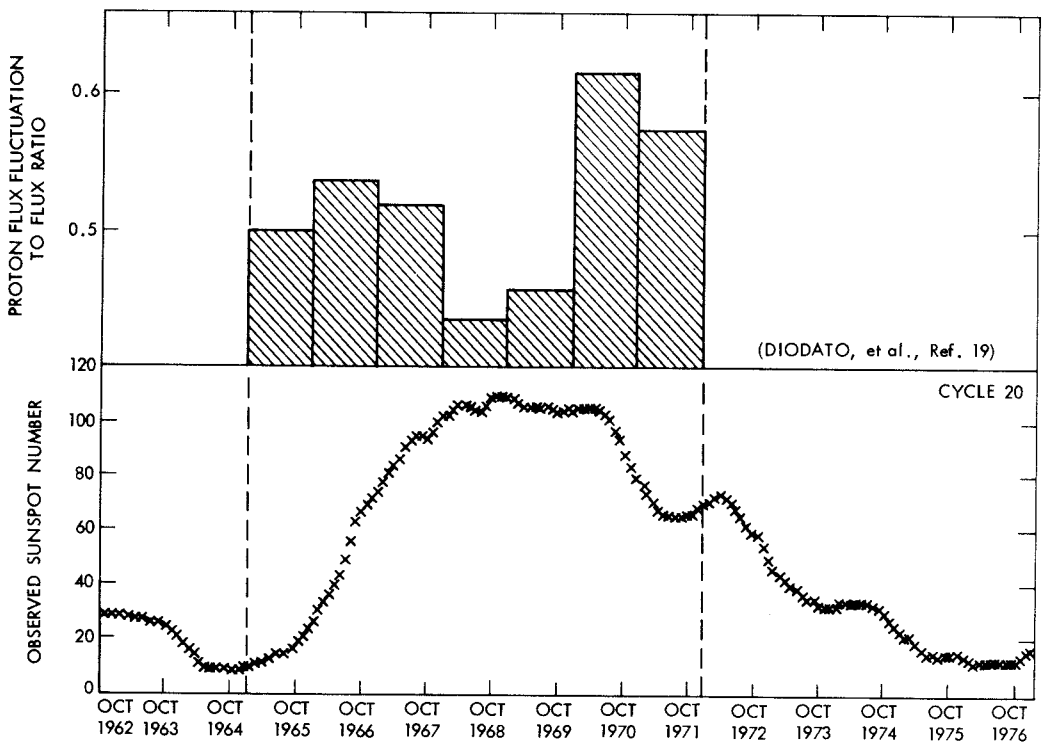

Fig. 8. Proton flux fluctuation to flux ratio, yearly average from 1965 to 1971 at 1 AU

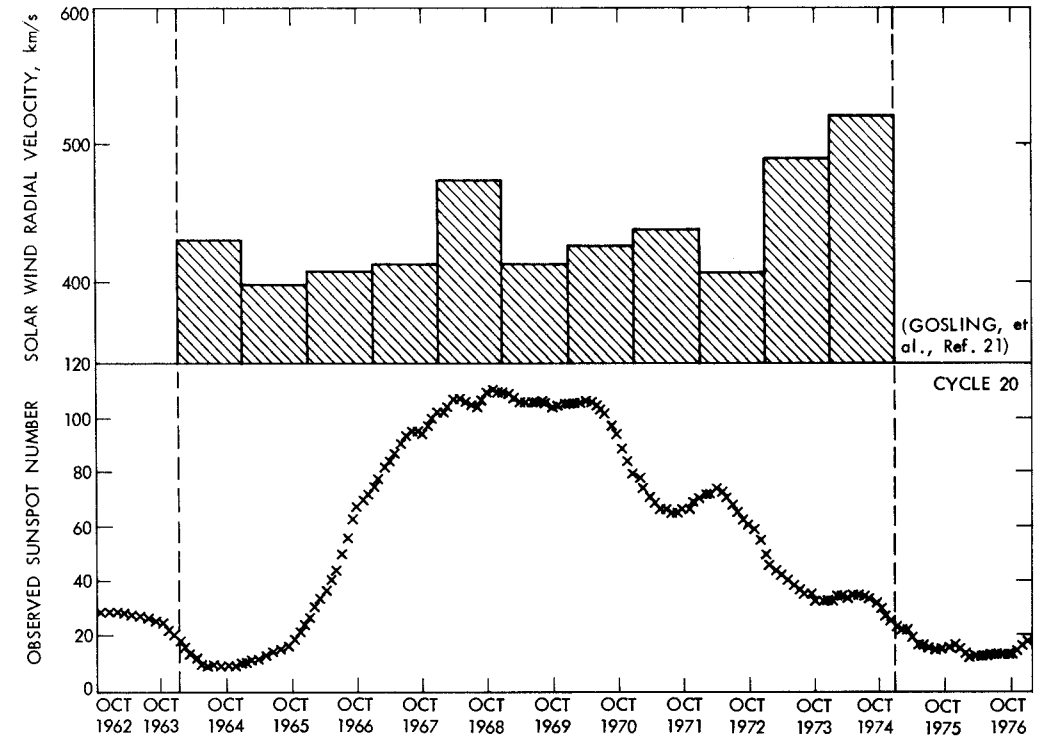

Fig. 9. Solar wind radial velocity yearly average at 1 AU, 1965 to 1974

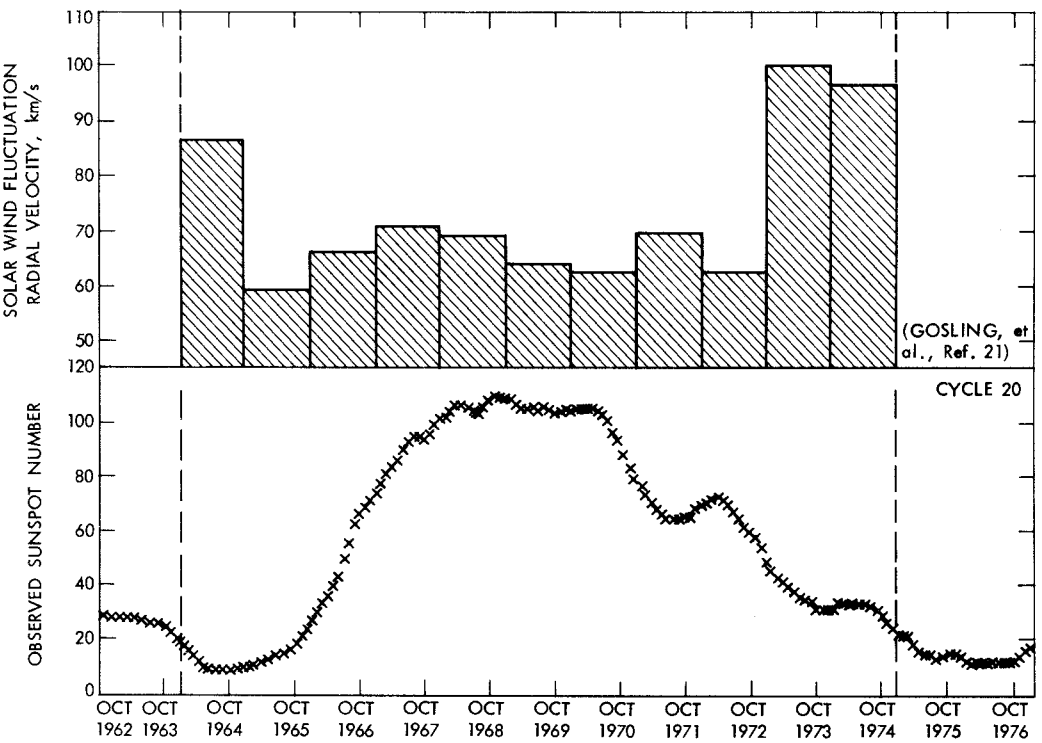

Fig. 10. Solar wind fluctuation radial velocity yearly average at 1 AU

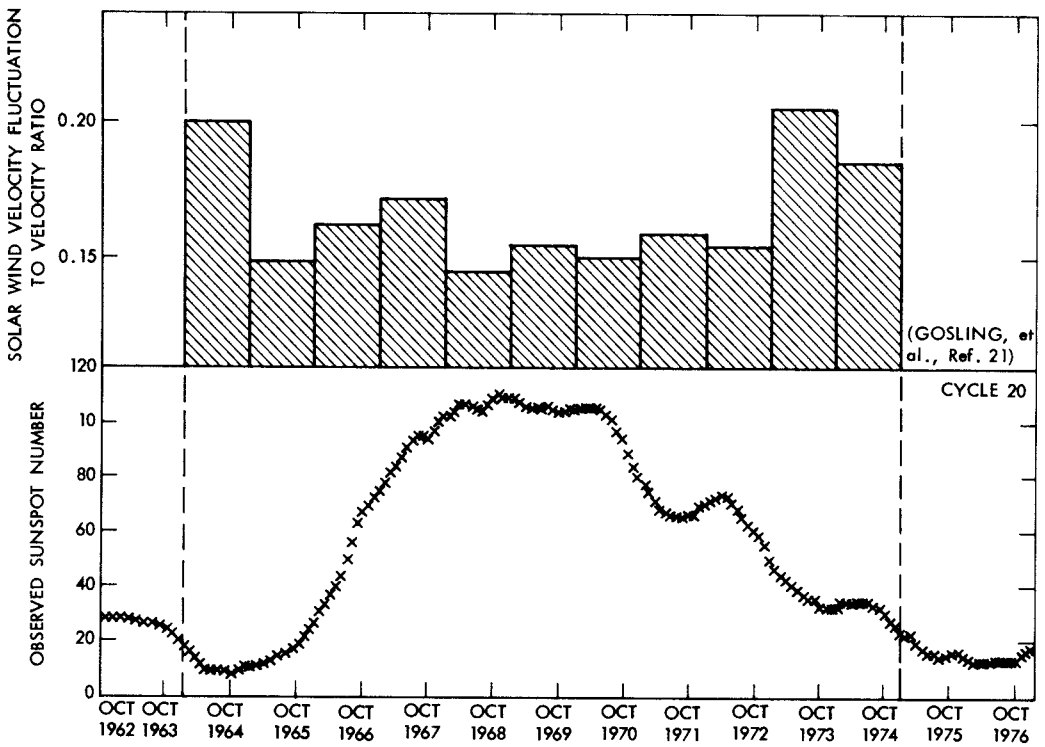

Fig. 11. Solar wind velocity fluctuation to velocity ratio, yearly average from 1964 to 1974 at 1 AU

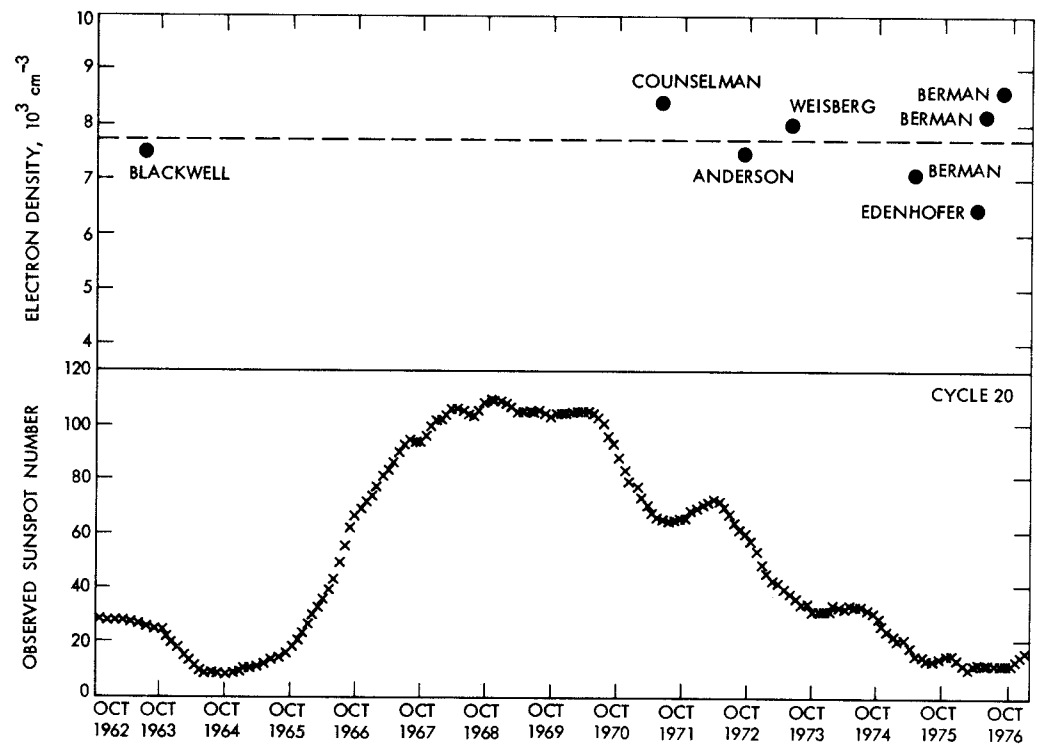

Fig. 12. Electron density model evaluations at $r = 10r_{\odot}$

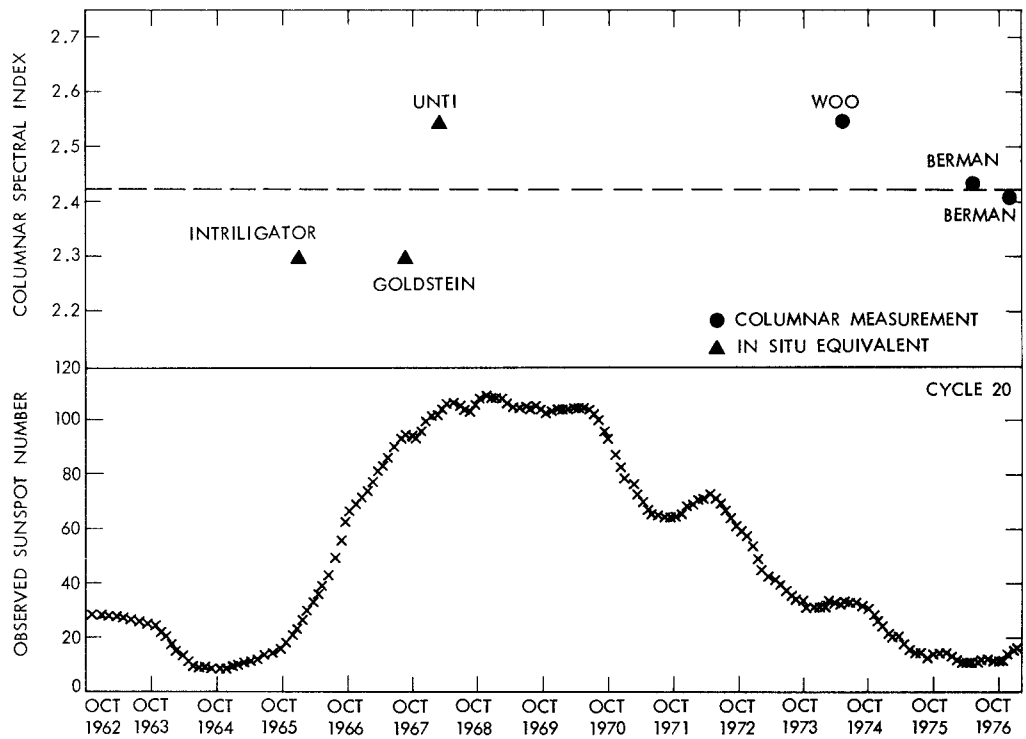

Fig. 13. Columnar (two-dimensional) density spectral inc